Excitation of Surface Acoustic Waves in a Z-section of Piezoelectric Crystals by the Electric Field of a Long Electrode

Igor V. Linchevskyi

Professor, Department of Physics and mathematics, National Technical University of Ukraine "Igor Sikorsky Kyiv Polytechnic Institute"37, Peremohy ave., Kyiv 03056, Ukraine

Abstract

The method for solving the homogeneous boundary-value problem of the dynamic elasticity theory is proposed, which allows one to obtain the general solutions describing the propagation of surface acoustic waves in Z–sections of single crystals of hexagonal syngony up to the constant factor. The plane problem of the excitation of surface acoustic waves in Z-sections of single crystals of hexagonal and cubic syngony is solved. The influence of the dimensions of the region of external forces existence on the levels of excited surface waves is shown. The concept of wave characteristic of a source of ultrasonic waves is introduced.

Keywords — *piezoelectric, surface acoustic waves, single crystals*

I. INTRODUCTION

The acoustoelectronic devices using surface acoustic waves (SAW) perform the signal filtration in real time [1], coding and decoding of the messages, implement the operation of transposition of the signal spectrum, and allow producing the frequency modulation and demodulation [2].

Owing to high portability [3] of the SAW devices and their implementation in the broad (up to units of gigahertz) frequency spectrum, they are promising components of electronic actuating mechanisms [4, 5], and telecommunication modulators [6, 7]. The usage of resonators on SAW allows creating the sensors of chemical [8–9], biochemical [10–13] and gas [14, 15] substances on their basis.

There are known methods of mathematical modeling which are based on the use of finite elements, the Green's function and the connected modes, which are widely used for the analysis and optimization of the SAW devices constructions [16–18].

The studies, the results **o**f which are presented in the papers [19–21], are based on the use of δ-sources. The results obtained using this technique can help the researcher to predict the capabilities and sensitivity of the device, and optimize the coordination of the SAW device with various samples of the materials under study and multilayer structures more accurately. However, the theoretical results obtained do not quite accurately correspond to the experimental data.

Other methods for analyzing SAW devices are based on the application of the impulse response, transfer matrices, and equivalent circuits, but they do not always give the desired coincidence of the theory with experimental results. Particularly large discrepancies between theoretical and experimental results arise when evaluating the electromechanical effect on the frequency characteristics of SAW devices [22–25].

Thus, the question of constructing of a mathematical model of SAW devices is remains relevant to this day.

II. METHODS

A. Problem statement and methods of solving

Suppose that an electrode is located on the surface $x_3 = 0$ of a Z-section of a piezoelectric single crystal (Fig. 1), the length of which significantly exceeds the maximum size 2ℓ of its rectangular cross section. The amplitude value $E^*(x_k)$ of the electric field vector of the electrode in its median part does not

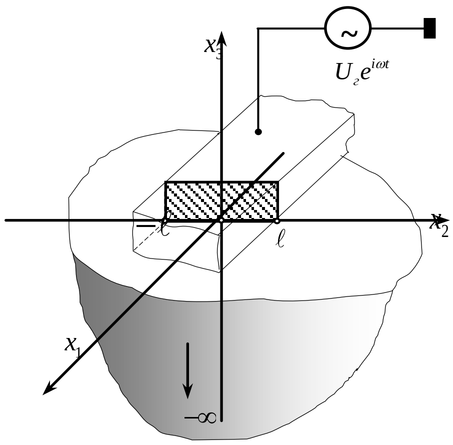

Fig 1: The design model of the

depend on the x_1 coordinate values and is completely determined by the two components $E_2^*(x_2, x_3)$ and $E_3^*(x_2, x_3)$.

The electric field of the electrode initates the inverse piezoelectric effect in the crystal. The amplitude values of the $\sigma_{nm}^*(x_k)$ components of the surface density of the Coulomb forces in a piezoelectric under the median part of the electrode are determined as follows

$$\sigma_{ij}\left(x_2, x_3\right) = e_{2ij} E_2\left(x_2, x_3\right) + e_{3ij} E_3\left(x_2, x_3\right), \quad (1)$$

where e_{kij} is the tensor component of the piezomodules.

The amplitude values of the $f_m^*\left(x_k\right)$ components of the vector of the volume density of the Coulomb forces under the median part of the long electrode are calculated by the formula

$$f_j\left(x_2, x_3\right) = \frac{\partial \sigma_{2j}\left(x_2, x_3\right)}{\partial x_2} + \frac{\partial \sigma_{3j}\left(x_2, x_3\right)}{\partial x_3}. \quad (2)$$

It follows from definitions (1) and (2) that

$$f_j\left(x_2, x_3\right) = e_{22j} \frac{\partial E_2\left(x_2, x_3\right)}{\partial x_2} + e_{32j} \frac{\partial E_3\left(x_2, x_3\right)}{\partial x_2} + e_{23j} \frac{\partial E_2\left(x_2, x_3\right)}{\partial x_3} + e_{33j} \frac{\partial E_3\left(x_2, x_3\right)}{\partial x_3}. \quad (3)$$

The electric field under the electrode initiates the inverse piezoelectric effect, and forces arise in the volume of the piezoelectric adjacent to the electrode. The resulting mechanical stress $\sigma_{ij}\left(x_k\right) e^{i\omega t}$ in the volume and on the surface of the piezoelectric is determined by the generalized Hooke's law, which is written for the amplitude values of physical fields in the form of

$$\sigma_{ij} = c_{ijkl}^E \frac{\partial u_l}{\partial x_k} - e_{kij} E_k, \quad (4)$$

where c_{ijkl}^E is the density module of the monocrystal; $u_l\left(x_k\right)$ is the amplitude of the k-th component of the displacement vector of the material particles of the piezoelectric single crystal, which varies in time according to the law $e^{i\omega t}$.

In corelation (3) and in all subsequent entries summation over twice-repeated indices is assumed by default.

The components of the displacement vector of the material particles of a piezoelectric satisfy Newton's second law: $\frac{\partial \sigma_{ij}}{\partial x_i} + \rho_0 \omega^2 u_j = 0$, where ρ_0 is the piezoelectric density.

Taking into account (1)

$c_{ijkl}^E \frac{\partial^2 u_k}{\partial x_l \partial x_i} + \rho_0 \omega^2 u_j = e_{kij} \frac{\partial E_k}{\partial x_i}$ is obtained.

The conditions at the piezoelectric-vacuum interface are of the following form

$$n_i \sigma_{ij} = 0 \, \forall x_k \in S, \quad (5)$$

where n_i is the i-th component of the vector of the external unit normal to the S surface of the piezoelectric.

The presence of the elastic forces and the Coulomb forces leads to an increase in the numerical values of the elastic moduli c_{33}^D. So, the elastic modulus c_{33}^E in a Z-section of a zincite single crystal (ZnO) can reach the value $c_{33}^D = c_{33}^E\left(1 + K_3^2\right)$, where $K_3^2 \cong 0.075$ is the square of the electromechanical coupling coefficient for the axial vibrations of the material particles of the piezoelectric. A possible increase in the elastic modulus c_{33}^E for a Z-section of a single-crystal CdS does not exceed $2.5 \cdot 10^{-2}$.

The solution of the boundary-value problem of the excitation of SAW by a system of bulk and surface loads makes it possible to approximatelydetermine the components of the displacement vector of the material particles of a piezoelectric, with an error of no more than K_3^2. Thus, the problem is reduced to finding general solutions to the system of equations

$$c_{ijkl}^E \frac{\partial^2 u_k^{(0)}}{\partial x_i \partial x_l} + \rho_0 \omega^2 u_j^{(0)} - f_j = 0 \, \forall x_k \in V, \quad (6)$$

which on the S surface of the piezoelectric ensure the fulfillment of the conditions (5).

The following notations are used in correlations (6): $f_j^* = e_{kij} \partial E_k^* / \partial x_i$ is the amplitude value of the j-th component of the bulk density vector of the Coulomb forces created by the electric field of an external source; V is the piezoelectric volume. The general solution to this problem allows us to determine the components of the displacement vector of material particles in the zeroth approximation.

B. Solutions in the zeroth approximation for a plane deformed state

In the case of a plane deformed state, a zeroth approximation $u_k^{(0)}\left(x_k\right) e^{i\omega t}$ to the exact values of the components $u_k\left(x_k\right) e^{i\omega t}$ of the displacement vector of material particles is determined by solving equations (6), which have the form:

$$c_{22}^E \frac{\partial^2 u_2^{(0)}\left(x_2, x_3\right)}{\partial x_2^2} + c_{44}^E \frac{\partial^2 u_2^{(0)}\left(x_2, x_3\right)}{\partial x_3^2} + \left(c_{23}^E + c_{44}^E\right) \frac{\partial^2 u_3^{(0)}\left(x_2, x_3\right)}{\partial x_2 \partial x_3} + \rho_0 \omega^2 u_2^{(0)}\left(x_2, x_3\right) = f_2^*\left(x_2, x_3\right), \quad (7)$$

$$c_{44}^E \frac{\partial^2 u_3^{(0)}\left(x_2, x_3\right)}{\partial x_2^2} + c_{33}^E \frac{\partial^2 u_3^{(0)}\left(x_2, x_3\right)}{\partial x_3^2} + \left(c_{23}^E + c_{44}^E\right) \frac{\partial^2 u_2^{(0)}\left(x_2, x_3\right)}{\partial x_2 \partial x_3} + \rho_0 \omega^2 u_3^{(0)}\left(x_2, x_3\right) =, = f_3^*\left(x_2, x_3\right) \quad (8)$$

$$c_{44}^E\left[\frac{\partial u_2^{(0)}(x_2,x_3)}{\partial x_3}+\frac{\partial u_3^{(0)}(x_2,x_3)}{\partial x_2}\right]\Bigg|_{x_3=0}-\sigma_{32}^*(x_2)=0, \quad (9)$$

$$\left[c_{23}^E\frac{\partial u_2^{(0)}(x_2,x_3)}{\partial x_2}+c_{33}^E\frac{\partial u_3^{(0)}(x_2,x_3)}{\partial x_3}\right]\Bigg|_{x_3=0}-\sigma_{33}^*(x_2)=0 \quad (10)$$

where $u_k^{(0)}(x_2,x_3),(k=2;3)$ is the aplitude value of a zeroth approximation to the exact value of the k-th component which varies in time according to the law $e^{i\omega t}$ of the displacement vector of the material particles of the piezoelectric; c_{22}^E, c_{23}^E, c_{33}^E, c_{44}^E and ρ_0 are elements of the matrix of elastic and density moduli of a piezoelectric single crystal; $f_k^*(x_2,x_3)$ and $\sigma_{3k}^*(x_2),(k=2;3)$ $(k=2;3)$ are the amplitude values of the components of the bulk density vector and the surface densities of external forces which vary in time according to the law $e^{i\omega t}$.

We assume that the loads created by external sources, i.e., the components $f_k^*(x_2,x_3)$ of the bulk density vector of the forces and the components of the tensor $\sigma_{3k}^*(x_2)$ of the surface density of external forces exist in the region $-\infty<x_1<\infty$ that has finite dimensions in the directions of the Ox_2 and Ox_3 axes of the coordinate system (x_1,x_2,x_3), the plane x_1Ox_2 of which is aligned with the Z-section surface of the single crystal. Bulk and surface loads satisfy the limit condition

$$\lim_{R\to\infty}\left[f_k^*(x_2,x_3),\sigma_{3k}^*(x_2)\right]=0, \quad (11)$$

where $R=\sqrt{x_2^2+x_3^2}$ is the distance from the area of the external forces existance.

These loads form wave fields of displacements of material particles, which satisfy the limiting conditions in the bulk and on the surface of the piezoelectric single crystal

$$\lim_{R\to\infty}\left[u_k^{(0)}(x_2,x_3),\ \frac{\partial u_k^{(0)}(x_2,x_3)}{\partial x_k}\right]=0. \quad (12)$$

The reduction of the system of equations (7) – (10) is performed using the integral Fourier transform along the x_2 coordinate.

We introduce the Fourier integral image of the physical field $\Phi(x_2,x_3)$ (this symbol denotes any one of the three quantities $u_k^{(0)}(x_2,x_3)$, $f_k^*(x_2,x_3)$ and $\sigma_{3k}^*(x_2)$) as a direct Fourier transform, i.e.

$$\Phi(\gamma,x_3)=\frac{1}{2\pi}\int_{-\infty}^{\infty}\Phi(x_2,x_3)e^{-i\gamma x_2}dx_2, \quad (13)$$

where the $\Phi(\gamma,x_3)$ symbol denotes any one of the three quantities $u_k^{(0)}(\gamma,x_3)$, $f_k^*(\gamma,x_3)$ and $\sigma_{3k}^*(\gamma)$; γ is the integral transformation parameter having the dimension of the wave number.

If the integral images $u_k^{(0)}(\gamma,x_3)$ of the components of the displacement vector are defined, then the transition to the originals $u_k^{(0)}(x_2,x_3)$ is carried out using the inverse Fourier transform, i.e.

$$u_k^{(0)}(x_2,x_3)=\int_{-\infty}^{\infty}u_k^{(0)}(\gamma,x_3)e^{i\gamma x_2}d\gamma. \quad (14)$$

The integral images from the derivatives of the components of the displacement vector on the x_2 coordinate are calculated taking into account the limiting condition (12). Wherein

$$\frac{1}{2\pi}\int_{-\infty}^{\infty}\frac{\partial u_k^{(0)}(x_2,x_3)}{\partial x_2}e^{-i\gamma x_2}dx_2=i\gamma u_k^{(0)}(\gamma,x_3),$$

$$\frac{1}{2\pi}\int_{-\infty}^{\infty}\frac{\partial^2 u_k^{(0)}(x_2,x_3)}{\partial x_2^2}e^{-i\gamma x_2}dx_2=-\gamma^2u_k^{(0)}(\gamma,x_3).$$

Taking into account the latest equalities, we come to the following formulation of the boundary-value problem (7) - (10) in terms of the integral Fourier images:

$$-\alpha^2k_{21}u_2^{(0)}(\gamma,x_3)+\frac{\partial^2u_2^{(0)}(\gamma,x_3)}{\partial x_3^2}+ \\ +i\gamma(1+\xi_2k_{21})\frac{\partial u_3^{(0)}(\gamma,x_3)}{\partial x_3}=\frac{f_2^*(\gamma,x_3)}{c_{44}^E}, \quad (15)$$

$$-\beta^2\xi_1k_{12}u_3^{(0)}(\gamma,x_3)+\frac{\partial^2u_3^{(0)}(\gamma,x_3)}{\partial x_3^2}+ \\ +i\gamma\xi_1(k_{12}+\xi_2)\frac{\partial u_2^{(0)}(\gamma,x_3)}{\partial x_3}=\frac{f_3^*(\gamma,x_3)}{c_{33}^E}, \quad (16)$$

$$\left[\frac{\partial u_2^{(0)}(\gamma,x_3)}{\partial x_3}+i\gamma u_3^{(0)}(\gamma,x_3)\right]\Bigg|_{x_3=0}-\frac{\sigma_{32}^*(\gamma)}{c_{44}^E}=0, \quad (17)$$

$$\left[i\gamma\xi_1\xi_2u_2^{(0)}(\gamma,x_3)+\frac{\partial u_3^{(0)}(\gamma,x_3)}{\partial x_3}\right]\Bigg|_{x_3=0}-\frac{\sigma_{33}^*(\gamma)}{c_{33}^E}=0, \quad (18)$$

where $\alpha^2=\gamma^2-k_1^2$; $k_1^2=\rho_0\omega^2/c_{22}^E$; $k_{21}=k_2^2/k_1^2=c_{22}^E/c_{44}^E$; $k_2^2=\rho_0\omega^2/c_{44}^E$; $\xi_2=c_{23}^E/c_{22}^E$; $\beta^2=\gamma^2-k_2^2$; $\xi_1=c_{22}^E/c_{33}^E$; $k_{12}=1/k_{21}$.

The general solution to the inhomogeneous boundary value problem (15) - (18) will be sought in the form:

$$u_2^{(0)}(\gamma,x_3)=\left[A+A(x_3)\right]e^{x_3r_1}+ \\ +\left[B+B(x_3)\right]e^{x_3r_3}+ \\ +C(x_3)e^{-x_3r_1}+D(x_3)e^{-x_3r_3}, \quad (19)$$

$$u_3^{(0)}(\gamma,x_3)=-\frac{i\alpha_{31}}{r_1}\left[A+A(x_3)\right]e^{x_3r_1}-$$
$$-\frac{i\alpha_{33}}{r_3}\left[B+B(x_3)\right]e^{x_3r_3}+$$
$$+\frac{i\alpha_{31}}{r_1}C(x_3)e^{-x_3r_1}+\frac{i\alpha_{33}}{r_3}D(x_3)e^{-x_3r_3},$$
(20)

where A and B are constants to be determined; $A(x_3)$, $B(x_3)$, $C(x_3)$ and $D(x_3)$ are variable constants that form a particular solution of equations (15) and (16); r_1 and r_3 are roots of the characteristic equation $H(r)=r^4-\Omega_1 r^2+\Omega_2=0$, where

$\Omega_1=\beta^2\xi_1 k_{12}+\alpha^2 k_{21}-\gamma^2\xi_1(k_{12}+\xi_2)(1+\xi_2 k_{21})$;

$\Omega_2=\alpha^2\beta^2\xi_1$;

$\alpha_{31}=(\alpha^2 k_{21}-r_1^2)/[\gamma(1+\xi_2 k_{21})]$;

$\alpha_{33}=(\alpha^2 k_{21}-r_3^2)/[\gamma(1+\xi_2 k_{21})]$;

$$r_{\binom{1,2}{3,4}}=\pm\sqrt{\frac{\Omega_1}{2}\pm\sqrt{\frac{(\xi_1\alpha^2-\beta^2)^2+2(\xi_1\alpha^2+\beta^2)\gamma^2 q+\gamma^4 q^2}{(\xi_1\alpha^2+\beta^2)^2}}}$$

$A(x_3)$, … , $D(x_3)$ constants satisfy the conditions:

$$A'(x_3)e^{x_3r_1}+B'(x_3)e^{x_3r_3}+C'(x_3)e^{-x_3r_1}+ \\ +D'(x_3)e^{-x_3r_3}=0, \qquad (21)$$

$$-\frac{i\alpha_{31}}{r_1}A'(x_3)e^{x_3r_1}-\frac{i\alpha_{33}}{r_3}B'(x_3)e^{x_3r_3}+ \\ +\frac{i\alpha_{31}}{r_1}C'(x_3)e^{-x_3r_1}+\frac{i\alpha_{33}}{r_3}D'(x_3)e^{-x_3r_3}=0, \qquad (22)$$

where the prime means the first derivative of the variable x_3.

Differentiating the proposed solutions (19) and (20) with respect to the variable x_3, and taking into account conditions (21) and (22), we find the first and second derivatives of the integral images of the displacement vector components of the material particles in the piezoelectric. After substituting the derivatives and expressions (21) and (22) into equations (15) and (16), we obtain the correlations:

$$r_1A'(x_3)e^{x_3r_1}+r_3B'(x_3)e^{x_3r_3}-r_1C'(x_3)e^{-x_3r_1}- \\ -r_3D'(x_3)e^{-x_3r_3}=f_2^*(\gamma,x_3)/c_{44}^E, \qquad (23)$$

$$-i\alpha_{31}A'(x_3)e^{x_3r_1}-i\alpha_{33}B'(x_3)e^{x_3r_3}-i\alpha_{31}C'(x_3)e^{-x_3r_1}- \\ -i\alpha_{33}D'(x_3)e^{-x_3r_3}=f_3^*(\gamma,x_3)/c_{33}^E, \qquad (24)$$

Conditions (21), (22) and equations (23), (24) form an inhomogeneous system of algebraic equations that are uniquely solved with respect to the first derivatives of the variable constants $A(x_3)$, … , $D(x_3)$. Integrating the quantities $A'(x_3)$, … , $D'(x_3)$ found from the system of equations (21) – (24), we obtain the following results:

$$A(x_3)=\frac{1}{2c_{33}^E(r_1^2-r_3^2)}\left[\begin{aligned}&\frac{(\alpha^2k_{21}-r_3^2)r_1}{\alpha^2\xi_1}\int_{-\infty}^{x_3}f_2^*(\gamma,x)e^{-xr_1}dx-\\&-i\gamma(1+\xi_2k_{21})\int_{-\infty}^{x_3}f_3^*(\gamma,x)e^{-xr_1}dx\end{aligned}\right]$$

$$B(x_3)=\frac{1}{2c_{33}^E(r_1^2-r_3^2)}\left[\begin{aligned}&-\frac{(\alpha^2k_{21}-r_1^2)r_3}{\alpha^2\xi_1}\int_{-\infty}^{x_3}f_2^*(\gamma,x)e^{-xr_3}dx+\\&+i\gamma(1+\xi_2k_{21})\int_{-\infty}^{x_3}f_3^*(\gamma,x)e^{-xr_3}dx\end{aligned}\right]$$

$$C(x_3)=\frac{1}{2c_{33}^E(r_1^2-r_3^2)}\left[\begin{aligned}&-\frac{(\alpha^2k_{21}-r_3^2)r_1}{\alpha^2\xi_1}\int_{-\infty}^{x_3}f_2^*(\gamma,x)e^{xr_1}dx-\\&-i\gamma(1+\xi_2k_{21})\int_{-\infty}^{x_3}f_3^*(\gamma,x)e^{xr_1}dx\end{aligned}\right]$$

$$D(x_3)=\frac{1}{2c_{33}^E(r_1^2-r_3^2)}\left[\begin{aligned}&\frac{(\alpha^2k_{21}-r_1^2)r_3}{\alpha^2\xi_1}\int_{-\infty}^{x_3}f_2^*(\gamma,x)e^{xr_3}dx+\\&+i\gamma(1+\xi_2k_{21})\int_{-\infty}^{x_3}f_3^*(\gamma,x)e^{xr_3}dx\end{aligned}\right]$$
. (25)

The constants A and B are determined from the boundary conditions (17) and (18). The expressions for their calculation have the form

$$A=A^*(\gamma)/\Delta_P(\gamma^2)-A(0), \\ B=B^*(\gamma)/\Delta_P(\gamma^2)-B(0), \qquad (26)$$

where

$$A^*(\gamma)=-\frac{r_3(1+\xi_2k_{21})}{k_{21}(\alpha^2+\xi_2r_3^2)}\left[\xi_1\xi_2-\frac{\alpha^2k_{21}-r_3^2}{\gamma^2(1+\xi_2k_{21})}\right]\frac{\sigma_{32}^*(\gamma)}{c_{44}^E}-$$
$$-\frac{i\sigma_{33}^*(\gamma)}{\gamma c_{33}^E}-C(0)\left\{\begin{aligned}&\xi_1\xi_2-\frac{\alpha^2k_{21}-r_1^2}{\gamma^2(1+\xi_2k_{21})}+\frac{r_3(\alpha^2+\xi_2r_1^2)}{r_1(\alpha^2+\xi_2r_3^2)}\\&\left[\xi_1\xi_2-\frac{\alpha^2k_{21}-r_3^2}{\gamma^2(1+\xi_2k_{21})}\right]\end{aligned}\right\}-$$
$$-2D(0)\left[\xi_1\xi_2-\frac{\alpha^2k_{21}-r_3^2}{\gamma^2(1+\xi_2k_{21})}\right];$$

$$B^*(\gamma)=\frac{r_3(1+\xi_2k_{21})}{k_{21}(\alpha^2+\xi_2r_3^2)}\left[\xi_1\xi_2-\frac{\alpha^2k_{21}-r_1^2}{\gamma^2(1+\xi_2k_{21})}\right]\frac{\sigma_{32}^*(\gamma)}{c_{44}^E}+$$
$$+\frac{i\sigma_{33}^*(\gamma)}{\gamma c_{33}^E}\frac{r_3(\alpha^2+\xi_2r_1^2)}{r_1(\alpha^2+\xi_2r_3^2)}+$$
$$+2C(0)\frac{r_3(\alpha^2+\xi_2r_1^2)}{r_1(\alpha^2+\xi_2r_3^2)}\left[\xi_1\xi_2-\frac{\alpha^2k_{21}-r_1^2}{\gamma^2(1+\xi_2k_{21})}\right]+$$
$$+D(0)\left\{\begin{aligned}&\xi_1\xi_2-\frac{\alpha^2k_{21}-r_1^2}{\gamma^2(1+\xi_2k_{21})}+\\&+\frac{r_3(\alpha^2+\xi_2r_1^2)}{r_1(\alpha^2+\xi_2r_3^2)}\left[\xi_1\xi_2-\frac{\alpha^2k_{21}-r_3^2}{\gamma^2(1+\xi_2k_{21})}\right]\end{aligned}\right\};$$

$$\Delta_P\left(\gamma^2\right)=\xi_1\xi_2-\frac{\alpha^2k_{21}-r_1^2}{\gamma^2\left(1+\xi_2k_{21}\right)}+$$
$$+\frac{r_3\left(\alpha^2+\xi_2r_1^2\right)}{r_1\left(\alpha^2+\xi_2r_3^2\right)}\left[\xi_1\xi_2-\frac{\alpha^2k_{21}-r_3^2}{\gamma^2\left(1+\xi_2k_{21}\right)}\right];$$

$A(0)$, $B(0)$, $C(0)$ and $D(0)$ are defined from the correlations (26) when $x_3=0$.

After calculations, the results of which are presented above, expressions (19) and (20) can be written in the following form:

$$u_2^{(0)}(\gamma,x_3)=\frac{A^*(\gamma)}{\Delta_P\left(\gamma^2\right)}e^{x_3r_1}+\frac{B^*(\gamma)}{\Delta_P\left(\gamma^2\right)}e^{x_3r_3}+ + R_2(\gamma,x_3), \quad (27)$$

$$u_3^{(0)}(\gamma,x_3)=-\frac{i\alpha_{31}}{r_1}\frac{A^*(\gamma)}{\Delta_P\left(\gamma^2\right)}e^{x_3r_1}- -\frac{i\alpha_{33}}{r_3}\frac{B^*(\gamma)}{\Delta_P\left(\gamma^2\right)}e^{x_3r_3}+R_3(\gamma,x_3), \quad (28)$$

The functions $R_2(\gamma,x_3)$ and $R_3(\gamma,x_3)$ have the following form in writing:

$$R_2(\gamma,x_3)=\left[A(x_3)-A(0)\right]e^{x_3r_1}+ +\left[B(x_3)-B(0)\right]e^{x_3r_3}+C(x_3)e^{-x_3r_1}+D(x_3)e^{-x_3r_3},$$

$$R_3(\gamma,x_3)=-\frac{i\alpha_{31}}{r_1}\left[A(x_3)-A(0)\right]e^{x_3r_1}-\frac{i\alpha_{33}}{r_3} \left[B(x_3)-B(0)\right]e^{x_3r_3}+\frac{i\alpha_{31}}{r_1}C(x_3)e^{-x_3r_1}+\frac{i\alpha_{33}}{r_3}D(x_3)e^{-x_3r_3}.$$

The constants A and B for $\gamma=\gamma_p$, where $\gamma_p=\omega/v_p$ is the wave number of a surface acoustic wave propagating with the speed v_p, turn to infinity, since $\Delta_P\left(\gamma_p^2\right)=0$. In the vicinity of a point $\gamma=\gamma_p$, the condition for the existence of a surface acoustic wave can be represented as an expansion in a Taylor series. Wherein

$$\Delta_P(\chi)=\Delta_P(\chi_p)+(\chi-\chi_p)\Delta_P'(\chi_p)+ +\frac{1}{2!}(\chi-\chi_p)^2\Delta_P''(\chi_p)+ +\ldots+\frac{1}{n!}(\chi-\chi_p)^n\Delta_P^{(n)}(\chi_p)+\ldots, \quad (29)$$

where $\chi=\gamma^2$ and $\chi_p=\gamma_p^2$; $\Delta_P'(\chi_p)=\partial\Delta_P(\chi)/\partial\chi\big|_{\chi=\chi_p}$ etc.

Since $\Delta_P(\chi_p)=0$, and $\Delta_P'(\chi_p)\neq0$, the expression (29) can be represented in the following form

$$\Delta_P(\chi)=(\chi-\chi_p)\Delta_P'(\chi_p)\left[\begin{matrix}1+\dfrac{1}{2!}(\chi-\chi_p)\dfrac{\Delta_P''(\chi_p)}{\Delta_P'(\chi_p)}+\\ +\ldots+\dfrac{1}{n!}(\chi-\chi_p)^{n-1}\dfrac{\Delta_P^{(n)}(\chi_p)}{\Delta_P'(\chi_p)}\end{matrix}\right]$$

Assuming the difference $\chi-\chi_p\equiv\gamma^2-\gamma_p^2$ to be a small number, we obtain

$$\Delta_P(\chi)\cong(\gamma-\gamma_p)(\gamma+\gamma_p)\Delta_P'(\chi_p). \quad (30)$$

It follows from expression (30) that, with the values of the integral transformation parameter $\gamma=\pm\gamma_p$, the constants A and B turn to infinity.

When performing the inverse integral transformation (14), it is necessary to satisfy the limit conditions (12). In this case, the wave number of the surface wave and is written in the form $\gamma_p^*=\gamma_p(1-i\delta)$, where $i=\sqrt{-1}$; δ is an arbitrarily small attenuation coefficient. Wherein, the calculation of the inverse Fourier transform (14) actually reduces to the calculation of the integral of the function, which is given in the complex plane ($\operatorname{Re}\gamma,\operatorname{Im}\gamma$).

Fig. 2 shows the complex plane and two points ($\gamma=\pm\gamma_p^*$) on it, at which the constants A and B turn to infinity, at which the integrand ceases to be an analytic function. These points can be excluded from the set of values of the complex parameter γ of the integral transformation bypassing them when performing integration over a circle of small radius $C_\rho=\rho e^{i\phi}$, where $\rho\to0$ is the radius of the circle; φ is zero to 2π polar angle When choosing a closed integration loop, it is necessary to ensure that the condition $\lim_{|x_3|\to\infty}u_k^{(0)}(x_2,x_3)=0$ is met. Thus, for the region $x_2>0$, i.e., for surface acoustic waves extending to the right of the region of existence of external forces, the integration contour should be in the upper half-plane of the complex plane ($\operatorname{Re}\gamma,\operatorname{Im}\gamma$). Wherein $e^{i\gamma x_2}=e^{ix_2\operatorname{Re}\gamma}e^{-x_2\operatorname{Im}\gamma}$ and where $x_2\to\infty$ the exponent $e^{i\gamma x_2}\to0$. For the region $x_2<0$, i.e., for waves that propagate to the left of the loading region, the closed integration loop should be in the lower half-plane of the complex plane of the integral transformation parameter.

C. *Example*

Let us consider the surface acoustic waves that carry energy in the positive direction of the Ox_2 coordinate axis.

For the longitudinal component of the displacement vector of material particles, the integral in the inverse Fourier transform (21) takes the following form

$$\oint_{C^{(+)}}\frac{1}{\Delta_P\left(\gamma^2\right)}\left[A^*(\gamma)e^{x_3r_1}+B^*(\gamma)e^{x_3r_3}\right]e^{i\gamma x_2}d\gamma+ +\oint_{K^{(+)}}R_2(\gamma,x_3)e^{i\gamma x_2}d\gamma=0, \quad (31)$$

where $C^{(+)} = AB + C_\rho + C_\infty^{(+)}$ and $K^{(+)} = AB + C_\infty^{(+)}$ are closed integration loops in the upper half-plane (Fig. 2) of the complex plane. The integrals on the vertical segments, which are located infinitely close to each other and connect the real axis (the

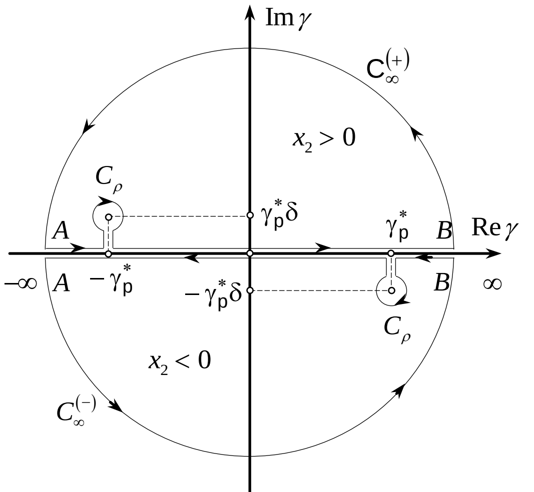

Fig 2: Integration contours when performing integral transformation (14)

segment AB in Fig. 2) of the complex plane with a small circle C_ρ, are mutually destroyed. The sum of the integrals on the left side of equality (31) is equal to zero by virtue of the general Cauchy theorem. Since there are no singular points inside closed loops $C^{(+)}$ and $K^{(+)}$, by virtue of the very Cauchy theorem, the integrals over closed loops $C^{(+)}$ and $K^{(+)}$ are equal to zero individually. The integrals over an arc of infinite radius $C_\infty^{(+)}$ in both integrals are equal to zero, since Jordan's lemma is valid.

As a result $\int_{-\infty}^{\infty} R_2(\gamma, x_3) e^{i\gamma x_2} d\gamma = 0$ and, consequently,

$$\int_{-\infty}^{\infty} u_2^{(0)}(\gamma, x_3) e^{i\gamma x_2} d\gamma = \tag{32}$$
$$= -\oint_{C_\rho} \frac{1}{\Delta_P(\gamma)} \begin{bmatrix} A^*(\gamma)e^{x_3 r_1} + \\ +B^*(\gamma)e^{x_3 r_3} \end{bmatrix} e^{i\gamma x_2} d\gamma$$

In the expression (30), a small quantity $\gamma + \gamma_p^*$ whose values are located on a circle C_ρ can be written in the form $\gamma + \gamma_p^* = \rho e^{i\phi}$. From this it follows that $d\gamma = i\rho e^{i\phi} d\phi$ and $\Delta_P(\chi) = -2\gamma_p^* \rho e^{i\phi} \Delta'_P(\chi_p)$. Assuming that wave numbers $\gamma \cong -\gamma_p^*$ are inside the contour C_ρ, expression (32) can be represented as follows

$$u_2^{(0)}(+x_2, x_3) = \frac{i e^{-i\gamma_p^* x_2}}{2\gamma_p^* \Delta'_P(\chi_p^*)} \begin{bmatrix} A^*(-\gamma_p^*)e^{x_3 r_1} + \\ +B^*(-\gamma_p^*)e^{x_3 r_3} \end{bmatrix} \int_0^{2\pi} d\phi =$$
$$= \frac{i\pi e^{-i\gamma_p^* x_2}}{\gamma_p^* \Delta'_P(\chi_p^*)} \left[A^*(-\gamma_p^*)e^{x_3 r_1} + B^*(-\gamma_p^*)e^{x_3 r_3} \right],$$

where $u_2^{(0)}(+x_2, x_3)$ is the amplitude value of the longitudinal component of the displacement vector of material particles in the surface wave propagating to the right of the region of existence of external forces; the roots of the characteristic equation r_1 and r_3 are determined at the value of the wave number $\gamma = -\gamma_p^*$.

Having completed the passage to the limit where $\delta \to 0$, i.e., eliminating the previously introduced extremely small attenuation, we obtain the final form of the expression for calculating the longitudinal component of the displacement vector of material particles

$$u_2^{(0)}(+x_2, x_3) = \frac{i\pi e^{-i\gamma_p x_2}}{\gamma_p \Delta'_P(\chi_p)} \begin{bmatrix} A^*(-\gamma_p)e^{x_3 r_1} + \\ + B^*(-\gamma_p)e^{x_3 r_3} \end{bmatrix}. \tag{33}$$

Similarly, we determine the vertical component

$$u_3^{(0)}(+x_2, x_3) =$$
$$= \frac{i\pi e^{-i\gamma_p x_2}}{\gamma_p \Delta'_P(\chi_p)} \begin{bmatrix} -\frac{i\alpha_{31}}{r_1} A^*(-\gamma_p)e^{x_3 r_1} - \\ -\frac{i\alpha_{33}}{r_3} B^*(-\gamma_p)e^{x_3 r_3} \end{bmatrix}. \tag{34}$$

For a surface wave, which propagates in the direction of increasing negative values of the x_2 coordinate, we obtain the following calculation formulas:

$$u_2^{(0)}(-x_2, x_3) = \frac{i\pi e^{i\gamma_p x_2}}{\gamma_p \Delta'_P(\chi_p)} \begin{bmatrix} A^*(\gamma_p)e^{x_3 r_1} + \\ + B^*(\gamma_p)e^{x_3 r_3} \end{bmatrix}, \tag{35}$$

$$u_3^{(0)}(-x_2, x_3) = \frac{i\pi e^{i\gamma_p x_2}}{\gamma_p \Delta'_P(\chi_p)} \begin{bmatrix} -\frac{i\alpha_{31}}{r_1} A^*(\gamma_p)e^{x_3 r_1} - \\ -\frac{i\alpha_{33}}{r_3} B^*(\gamma_p)e^{x_3 r_3} \end{bmatrix}. \tag{36}$$

Since where $\gamma = \pm\gamma_p$

$$\xi_1\xi_2 - \frac{\alpha^2 k_{21} - r_3^2}{\gamma_p^2(1 + \xi_2 k_{21})} =$$
$$= \frac{r_1(\alpha^2 + \xi_2 r_3^2)}{r_3(\alpha^2 + \xi_2 r_1^2)} \left[\xi_1\xi_2 - \frac{\alpha^2 k_{21} - r_1^2}{\gamma_p^2(1 + \xi_2 k_{21})} \right],$$ there

$$B^*(\pm\gamma_p) = -\frac{r_3(\alpha^2 + \xi_2 r_1^2)}{r_1(\alpha^2 + \xi_2 r_3^2)} A^*(\pm\gamma_p). \tag{37}$$

Taking into account the expressions (37) corrections (33) – (36) can be represented in the following way:

$$u_2^{(0)}\left(\pm x_2, x_3\right) = A\left(\mp\gamma_p\right)U_2\left(\gamma_p, x_3\right)e^{\mp i\gamma_p x_2},$$

$$u_3^{(0)}\left(\pm x_2, x_3\right) = \mp iA\left(\mp\gamma_p\right)U_3\left(\gamma_p, x_3\right)e^{\mp i\gamma_p x_2},$$

where $A\left(\mp\gamma_p\right)$ is the amplitude factor of the surface acoustic wave, and $A\left(\pm\gamma_p\right) = \dfrac{i\pi A^*\left(\pm\gamma_p\right)}{\gamma_p \Delta_P'\left(\chi_p\right)}$;

$$A^*\left(\pm\gamma_p\right) = -\frac{r_3\left(1+\xi_2 k_{21}\right)}{k_{21}\left(\alpha^2+\xi_2 r_3^2\right)}\left[\xi_1\xi_2 - \frac{\alpha^2 k_{21}-r_3^2}{\gamma_p^2\left(1+\xi_2 k_{21}\right)}\right]$$

$$\frac{\sigma_{32}^*\left(\pm\gamma_p\right)}{c_{44}^E} \mp \frac{i}{\gamma_p}\frac{\sigma_{33}^*\left(\pm\gamma_p\right)}{c_{33}^E} -$$

$$-2C(0)\left[\xi_1\xi_2 - \frac{\alpha^2 k_{21}-r_1^2}{\gamma_p^2\left(1+\xi_2 k_{21}\right)}\right] -$$

$$-2D(0)\left[\xi_1\xi_2 - \frac{\alpha^2 k_{21}-r_3^2}{\gamma_p^2\left(1+\xi_2 k_{21}\right)}\right];$$

$$C(0) = \frac{1}{2c_{33}^E\left(r_1^2-r_3^2\right)}$$

$$\left[-\frac{\left(\alpha^2 k_{21}-r_3^2\right)r_1}{\alpha^2\xi_1}\int_{-\infty}^{0} f_2^*\left(\pm\gamma_p, x\right)e^{xr_1}dx \mp \mp i\gamma_p\left(1+\xi_2 k_{21}\right)\int_{-\infty}^{0} f_3^*\left(\pm\gamma_p, x\right)e^{xr_1}dx\right]$$

$$D(0) = \frac{1}{2c_{33}^E\left(r_1^2-r_3^2\right)}$$

$$\left[\frac{\left(\alpha^2 k_{21}-r_1^2\right)r_3}{\alpha^2\xi_1}\int_{-\infty}^{0} f_2^*\left(\pm\gamma_p, x\right)e^{xr_3}dx \mp \pm i\gamma_p\left(1+\xi_2 k_{21}\right)\int_{-\infty}^{0} f_3^*\left(\pm\gamma_p, x\right)e^{xr_3}dx\right]$$

$$\left\{\begin{array}{c}\sigma_{3k}^*\left(\pm\gamma_p\right)\\ f_k^*\left(\pm\gamma_p, x_3\right)\end{array}\right\} = \frac{1}{2\pi}\int_{-\infty}^{\infty}\left\{\begin{array}{c}\sigma_{3k}^*\left(x_2\right)\\ f_k^*\left(x_2, x_3\right)\end{array}\right\}e^{\mp i\gamma_p x_2}dx_2;$$

$U_k\left(\gamma_p, x_3\right)$ $(k=2,3)$ are eigenfunctions of a homogeneous boundary value problem defined by the following expressions

$$U_2\left(\gamma_p, x_3\right) = e^{x_3 r_1} - \frac{r_3\left(\alpha^2+r_1^2\xi_2\right)}{r_1\left(\alpha^2+r_3^2\xi_2\right)}e^{x_3 r_3};$$

$$U_3\left(\gamma_p, x_3\right) = \frac{\alpha^2 k_{21}-r_1^2}{\gamma_p r_1\left(1+\xi_2 k_{21}\right)}$$

$$\left[e^{x_3 r_1} - \frac{\left(\alpha^2 k_{21}-r_3^2\right)\left(\alpha^2+r_1^2\xi_2\right)}{\left(\alpha^2 k_{21}-r_1^2\right)\left(\alpha^2+r_3^2\xi_2\right)}e^{x_3 r_3}\right]$$

III. RESULTS OF THE RESEARCH AND THEIR DISCUSSION

Suppose that a normal voltage $\sigma_{33}^*\left(x_2\right) = \sigma_0 f\left(x_2\right)e^{i\omega t}$ acts on the surface of a crystal in a strip with the width of 2ℓ, where the distribution function is $f\left(x_2\right) = 1 \;\forall\; x_2 \in [-\ell, \ell]$ and $f\left(x_2\right) = 0 \;\forall\; x_2 \notin [-\ell, \ell]$. In this case, the integrated image of the surface load is

$$\sigma_{33}^*\left(\pm\gamma_p\right) = \frac{\sigma_0}{2\pi}\int_{-\ell}^{\ell} e^{\mp i\gamma_p x_2}dx_2 = \frac{\sigma_0\ell}{\pi}\frac{\sin\gamma_p\ell}{\gamma_p\ell}.$$

The amplitude multiplier of the surface wave is $A\left(\pm\gamma_p\right) = \pm\dfrac{\sigma_0\ell}{\gamma_p^2\Delta_P'\left(\chi_p\right)c_{33}^E}W\left(\gamma_p, \ell\right)$, where $W\left(\gamma_p, \ell\right) = \sin\gamma_p\ell/\left(\gamma_p\ell\right)$.

The components of the displacement vector of material particles to the right ($+x_2$) and left ($-x_2$) of the strip $-\ell \le x_2 \le \ell$ are determined by the following expressions:

$$u_2^{(0)}\left(\pm x_2, x_3\right) = \mp\frac{\sigma_0\ell}{\gamma_p^2\Delta_P'\left(\chi_p\right)c_{33}^E}W\left(\gamma_p, \ell\right)U_2\left(\gamma_p, x_3\right)e^{\mp i\gamma_p x_2},$$

$$u_3^{(0)}\left(\pm x_2, x_3\right) = \frac{\sigma_0\ell e^{i\pi/2}}{\gamma_p^2\Delta_P'\left(\chi_p\right)c_{33}^E}W\left(\gamma_p, \ell\right)U_2\left(\gamma_p, x_3\right)e^{\mp i\gamma_p x_2}.$$

It can be seen that the amplitude values of the components of the displacement vector are directly proportional to the values of the function $W\left(\gamma_p, \ell\right)$, which decreases with increasing the dimensionless wave number $\gamma_p\ell$ and, most importantly, vanishes at

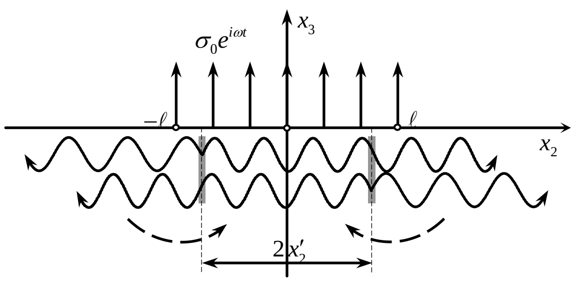

Fig 3: To an explanation of the physical meaning of the wave characteristic of the source of surface acoustic waves. ℓ - electrode boundaries

$\gamma_p\ell = \pi m$ $(m = 1, 2, \ldots)$, when the surface wave length λ_p is a multiple of the size of the loading region, i.e. $\lambda_p = 2\ell/m$. In accordance with the values of the function $W\left(\gamma_p, \ell\right)$, the displacement of material particles in the front of the surface acoustic wave changes.

Consider a small section of the elastic half-space (Fig. 3), bounded by planes $x_2' \pm \Delta x_2$, located in the field of external forces in the region $(0 \le x_2' \le \ell)$. Material particles of this section of the elastic half-space move under the action of external forces (the trajectory of motion at some fixed point in time is indicated with dashed arrows). The selected portion of the elastic half-space can be considered as some elementary emitter that generates a stationary displacement field, which is characterized by a stationary phase distribution along the Ox_2 coordinate axis.

Another small area bounded by planes $-x_2' \pm \Delta x_2$ $(-\ell \le x_2' \le 0)$ can be interpreted as another elementary radiator, with a stationary phase distribution along the Ox_2 coordinate axis. Between these two phase distributions there is a constant phase shift, which is proportional to $2\gamma_p x_2'$, and depending on the frequency of oscillations and the distance between the radiating sections, it can acquire values in the range from 0 to 2π. Depending on the value of this phase shift, either mutual suppression of the radiation of two sections of the half-space symmetrically located relative to the plane $x_2 = 0$ or such addition of these fields that maximizes the resulting value of the displacement of material particles can be observed. For some values of the frequency (dimensionless wave number), the phase difference between stationary fields emitted by various elementary sections located symmetrically relative to the plane $x_2 = 0$, reaches such a value that complete mutual compensation of displacements of material particles occurs, which are located outside the region of loading of the surface of the piezoelectric crystal by external forces. This situation corresponds to zero displacement amplitudes and periodically repeats with the increasing frequency.

The function $W(\gamma_p, \ell)$ determines the frequency response of the considered source of elastic disturbances. For the same frequency values and sizes of the loading region, the amplitudes of surface acoustic waves will be different for crystals with different material parameters. Obviously, since the values of the function $W(\gamma_p, \ell)$ are entirely determined by the values of the wave number γ_p. With this in mind, it seems appropriate to call the function $W(\gamma_p, \ell)$ the wave characteristic of the source of ultrasonic waves.

IV. CONCLUSIONS

The plane problem of the excitation of surface acoustic waves in Z-sections of single crystals of hexagonal and cubic syngony is solved. The influence of the dimensions of the region of external forces existence on the levels of excited surface waves is shown. The concept of wave characteristic of a source of ultrasonic waves is introduced.

REFERENCES

[1] Morgan D., Surface acoustic wave filters with applications to electronic communications and signal processing. Elsevier, 2007, 448.

[2] T. Wang , R. Green, R. Guldiken , J. Wang, S. Mohapatra, S. S. Mohapatra, Finite Element Analysis for Surface AcousticWaveDevice Characteristic Properties and Sensitivity. Sensors, vol. 19, no. 8., p.1749., 2019, doi:10.3390/s19081749.

[3] W. Buff , F. Plath, O. Schmeckebier, M. Rusko, T. Vandahl, H. Luck, F. Moller, D. Malocha, Remote sensor system using passive SAW sensors. Proceeding of the Utrasonics Symposium, 31 October –3 November, Cannes, France, pp. 585–588, 1994.

[4] R. Guldiken, M.C. Jo, N.D. Gallant, U. Demirci, J. Zhe, Size-Based Acoustic Particle Separation , Sensors, vol. 12, no.1, pp. 905–922.,2012. doi.org/10.3390/s120100905

[5] T. Wang, Q. Ni, N.B. Crane, R. Guldiken, Surface acoustic wave based pumping in a microchannel / Microsyst. Technol., vol.23, no.5., pp.1-8. doi: 10.1007/s00542-016-2880-9, 2016.

[6] J. R. Gell, M.B. Ward, R.J. Young, R.M. Stevenson, P. Atkinson, D. Anderson, G. Jones, D.A. Ritchie, A.J., Shields, Modulation of single quantum dot energy levels by a surface-acoustic-wave. Appl. Phys. Lett., vol. 93. , pp. 081115, 2008. doi.org/10.1063/1.2976135.

[7] Aigner R., SAW and BAW technologies for RF filter applications: A review of the relative strengths and weaknesses. 2008 IEEE Ultrasonics Symposium, 2–5 November 2008, Beijing, China: proc. symp. 2008., pp. 582–589, 2008.

[8] Mujahid , F. L. Dickert, Surface acousticwave (saw) for chemical sensing applications of recognition layers, Sensors , vol.17, no.12, p.2716, 2017. doi:10.3390/s17122716 .

[9] G.F. Fine, L.M. Cavanagh, A. Afonja, R. Binions, Metal oxide semi-conductor gas sensors in environmental monitoring, Sensors, vol. 10, no.6, pp. 5469–5502, 2010. doi.org/10.3390/s100605469.

[10] I.A. Casalinuovo, D. Di Pierro, E. Bruno, P. Di Francesco, M. Coletta, Experimental use of a new surface acoustic wave sensor for the rapid identification of bacteria and yeasts, Lett. App. Microbiol., vol.42, no.1., pp. 24–29, 2006. doi.org/10.1111/j.1472-765X.2005.01792.x.

[11] O. Onen, A. Sisman, N.D. Gallant, P. Kruk, R.A. Guldiken, A urinary bcl-2 surface acoustic wave biosensor for early ovarian cancer detection, Sensors, vol.12, no.6., pp. 7423–7437, 2012. doi.org/10.3390/s120607423.

[12] O. Onen, A.A. Ahmad, R. Guldiken, N.D. Gallant Surface Modification on Acoustic Wave Biosensors for Enhanced Specificity, Sensors, vol. 12, no. 9., pp. 12317–12328, 2012. doi.org/10.3390/s120912317.

[13] Y. Zhang, F. Yang, Z. Sun, Y.-T. Li, G.-J. Zhang, A surface acoustic wave biosensor synergizing DNA-mediated in situ silver nanoparticle growth for a highly specific and signal-amplified nucleic acid assay, Analyst, vol. 142. no.8, pp. 3468–3476, 2017. doi: 10.1039 / c7an00988g.

[14] W. Jakubik, P. Powro´znik, J. Wrotniak, J, M. Krzywiecki, Theoretical analysis of acoustoelectrical sensitivity in SAWgas sensors with single and bi-layer structures, Sens. Actuators B: Chem., vol.236, no.11, pp.1069–1074, 2016. doi.org/10.1016/j.snb.2016.05.157.

[15] A. Marcu, C. Viespe, Surface Acoustic Wave Sensors for Hydrogen and Deuterium Detection, Sensors, 2017. vol. 17, no.6., pp. 1417, 2017. doi.org/10.3390/s17061417.

[16] K. Hashimoto, G. Endoh, M. Yamaguchi, Coupling-of-modes modelling for fast and precise simulation of leaky surface acoustic wave devices, 1995 IEEE Ultrasonics:

Symposium, 7–10 November 1995, Seattle, WA, USA, : proc. of conf., vol.1. , pp. 251–256, 1995.

[17] J.H. Kuypers, A.P. Pisano, Green's function analysis of Lamb wave resonators, IEEE Ultrasonics: Symposium, 2–5 November 2008, Beijing, : proc. of conf. , pp. 1548–1551, 2008. doi: 10.1109/ultsym.2008.0377.

[18] Tewary V.K., Green's-function method for modeling surface acoustic wave dispersion in anisotropic material systems and determination of material parameters, Wave Motion.,vol. 40, no.4., pp. 399–412, 2004. doi.org/10.1016/j.wavemoti.2004.02.007.

[19] Xu G., Direct finite-element analysis of the frequency response of a Y-Z lithium niobate SAW filter, Smart Mater. Struct., vol.9, no.6, pp. 973–980, 2000. doi: 10,1088 / 0964-1726 / 9 / 6/401.

[20] K.M.M. Kabir, G.I. Matthews, Y.M. Sabri, S.P. Russo, S.J. Ippolito, S.K. Bhargava, Development and experimental verification of a finite element method for accurate analysis of a surface acoustic wave device, Smart Mater. and Struct., vol. 25, P.035040, 2016.

[21] M. EL. Gowini, W.A. Moussa, Finite Element Model of a MEMS-based Surface Acoustic Wave Hydrogen Sensor, Sensors, vol.10, no.2, pp.1232–1250, 2010. doi: 10.3390/s100201232.

[22] K.-C. Park, J. R.Yoon, Transmission Line Matrix Modeling for Analysis of Surface Acoustic Wave Hydrogen Sensor, Jpn. J. Appl. Phys.,vol. 50, no.7S. — 07HD06, 2011.

[23] T. Kojima, H. Obara, K. Shibayama, Investigation of Impulse Response for an Interdigital Surface-Acoustic-Wave Transducer., Jpn. J. Appl. Phys., vol.29, no.1, p.125, 1990.

[24] Hoang T., SAW Parameters Analysis and Equivalent Circuit of SAW Device, Acoustic Waves—From Microdevices to Helioseismology, In Tech: Rijeka, Croatia, 2011. doi: 10.5772/19910.

[25] T. Kojima, K. Shibayama, An analysis of an equivalent circuit model for an interdigital surface-acoustic-wave transducer, Jpn. J. Appl. Phys., vol. 27, pp.163-165., 1998.